research article

The "question-mark" MR anatomy of the cervico-thoracic ganglia complex: can it help to avoid mistaking it for a malignant lesion on ^{68}Ga-PSMA-11 PET/MR?

Ewa J. Bialek[1,2], Bogdan Malkowski[1,3]

[1] Department of Nuclear Medicine, The Franciszek Lukaszczyk Oncology Centre, Bydgoszcz, Poland
[2] Department of Nuclear Medicine, Military Institute of Medicine, Warsaw, Poland
[3] Department of Positron Emission Tomography and Molecular Diagnostics, Collegium Medicum of Nicolaus Copernicus University, Bydgoszcz, Poland

Radiol Oncol 2019; 53(4): 407-414.

Received 2 April 2019
Accepted 9 September 2019

Correspondence to: Bogdan Malkowski, Department of Nuclear Medicine, Oncology Centre, ul. dr I. Romanowskiej 2, 85-796 Bydgoszcz, Poland. E-mail: bmalkowski@mp.pl

Disclosure: No potential conflicts of interest were disclosed.

Background. Detectable uptake of ^{68}Ga-PSMA-ligands in sympathetic ganglia may potentially lead to mistaking them for malignant lesions. Our aim was to investigate the anatomy of cervico-thoracic-ganglia-complex (CTG-C) in the MR part of multimodal ^{68}Ga-PSMA-11 PET/MR imaging, in view of PET factors hindering its proper identification.

Patients and methods. In 106 patients, 212 sites of the CTG-C were retrospectively reviewed to assess the radiotracer uptake (SUV_{max}), size, shape, position, symmetry of location and visual uptake intensity. Asymmetry of PSMA-ligand uptake and increased uptake were regarded as risk factors of malignancy.

Results. In 66.0% left (L) and 53.8% right (R) CTG-C we noticed configurations, resembling the shape of an exclamation-mark, a question-mark, or its part (called "typical"). Tumor-like CTG-C shapes (oval, binodular or longitudinal) were detected in 28.3% L-CTG-C and in 40.6% R-CTG-C. When visual assessment of PET suggested malignancy, the recognition of "typical" shape of underlying CTG-C on MR generated a rise in the accuracy of their proper identification (from 34.4% to 75%, $\chi 2(1) = 70.4$; $p < 0.001$). Recognizing the shape of the CTG-C as "typical" in MR allowed us to classify as "not-suspicious" 61.9% of all CTG-C which were treated as "suspicious" after sole PET assessment.

Conclusions. The characteristic shape of cervico-thoracic-ganglia-complex (resembling a question-mark, or its part) helps in proper recognition of CTG-C on multimodal whole-body ^{68}Ga-PSMA-ligand PET/MR imaging, when detectable uptake might lead to considering pathology.

Key words: stellate ganglion; cervico-thocaracic ganglion; ^{68}Ga-PSMA; metastasis; lymph node; PET/MR; prostate; oncology

Introduction

Ganglia are consolidated parts of the sympathetic network located symmetrically along the spine. At the border of the chest and neck, the sympathetic inferior cervical ganglion (ICG) and the first thoracic ganglion (T1), may fuse to form a relatively large, variedly shaped, cervico-thoracic ganglion (CTG), called also the stellate ganglion (SG) (Figure 1A). Reported percentages of such fusions were scattered from 28% by Raveendran and Kamalamma[1] through about 82–83%[2,3]; up to 100% according to Hoffman.[4]

The exact location of CTG/SG had been studied in detail on cadavers[1-3,5-7] to find reliable anatomic landmarks for the needs of their therapeutic block

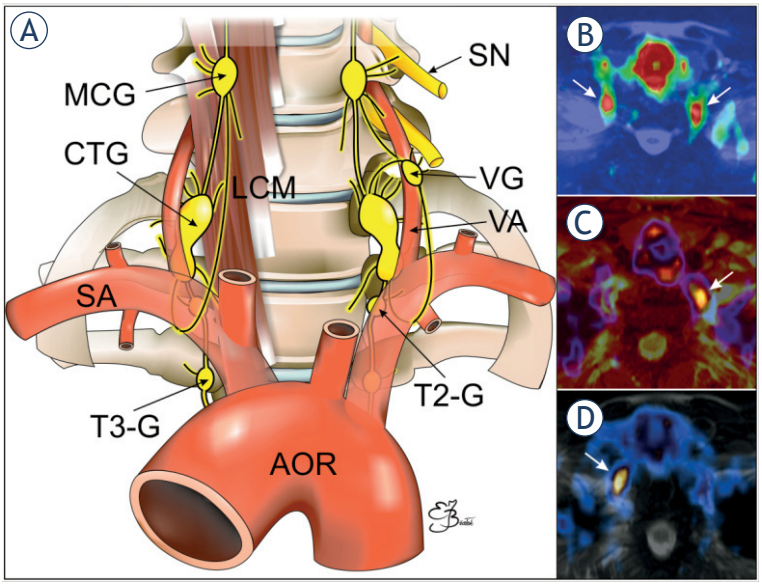

FIGURE 1. The scheme of the location of the sympathetic cervico-thoracic ganglia (CTG) and their surroundings **(A)** and examples of elevated PSMA-ligand uptake, potentially suggesting malignancy in both CTG complexes **(B)**, in the left CTG **(C)** and in the right CTG **(D)** on fused PET/MR T2-weighted images presented with application of different colour maps.

AOR = aortic arch; LCM = longus colli muscle; MCG = middle cervical sympathetic ganglion; SA = subclavian artery; SN = spinal nerve; T2-G = 2nd thoracic sympathetic ganglion; T3-G = 3rd thoracic sympathetic ganglion; VA = vertebral artery; VG = vertebral sympathetic ganglion

or ablation to relieve pain, in different diseases including cardio-vascular and post-traumatic stress disorder[8-10] or to assist avoiding their iatrogenic damage during surgery.

For a long time CTG/SG were not possible to be detected on any imaging because of their relatively small size. The first imaging study claims to be the magnetic resonance (MR) one, by Hogan and Ericson.[11] However, even when CTG/SG started to be visible on imaging, their proper classification was not essentially crucial from oncological point of view, as erroneous taking them for normal or benign lymph nodes did not generally cause any harm to the patient.

The circumstances changed after the introduction of a new radiotracer to multimodal positron emission tomography/computer tomography (PET/CT) imaging. The prostate specific membrane antigen (PSMA)-targeted radiotracers labelled with radioactive gallium (Ga-68) used for the primary staging and follow-up of prostate cancer patients, turned out to gather also in sympathetic ganglia, including CTG/SG.[12-15] In such circumstances, the relatively small size of CTG/SG does not exclude them from suspicion of malignancy, when they show the radiotracer uptake on PET, because ^{68}Ga-PSMA ligand (PET/CT) has the functional potential do detect micrometastases even in non-enlarged, and therefore missed on only morphological CT assessment, lymph nodes.[16,17]

Detection of uptake in CTG/SG on multimodal PET/CT imaging, causes the possibility of mistaking them for malignant lesions, primarily metastatic lymph nodes[12,13,15], which may lead to erroneous patient management and unnecessary treatment. The proposed hints for avoiding harmful misdiagnosis included the awareness of a possible pitfall, the anatomic location of CTG/SG[13], CTG/SG special shape, *i.e.* often met band- and tear-drop configuration, and significantly higher intensity of uptake than in prostate cancer metastatic lymph nodes.[15] However, the mentioned papers dealt with PET imaging combined with CT. In our study we have taken into consideration the MR-based multimodal PET imaging in order to check the shape of cervico-thoracic ganglia complex (CTG-C), in the view of PET factors hindering its proper identification (Figure 1B-D), including fused CTG/SG, not-fused CTG/SG and their connections with adjacent sympathetic ganglia if visible.

Patients and methods

The retrospective analysis of 212 sites of a CTG complex was undertaken in 106 patients undergoing whole body ^{68}Ga-PSMA-11 PET/MR examination. The retrospective study was performed in accordance with the principles of the 1964 Declaration of Helsinki and all subsequent revisions and with national regulations. All patients had provided routine written informed consent before each examination.

The patients were males (age range 40–78 years, mean 63.70 ± 6.86 years; weight range 59–115 kg, mean 86 ± 29 kg) referred for routine primary staging or follow-up of prostate cancer between November 2015 and February 2018. All exams were performed using a multimodal PET/MR system (Biograph mMR scanner, Siemens, Germany, based on the 3T MR platform). All patients underwent the whole body MR and the whole body PET imaging about 83.04±19.96 minutes (range, 50–143 minutes) after injection of 168.43 ± 17.69 MBq (range, 115–210 MBq) of ^{68}Ga-PSMA-11.

The procedure of ^{68}Ga-PSMA-11 preparation and the imaging protocol was the same as already described in Bialek and Malkowski.[18] ^{68}Ga-PSMA-11 was synthesized as follows. ^{68}Ge/^{68}Ga generator (Eckert & Ziegler Rdiopharma GmbH, Berlin, Germany) was eluted with 5ml of sterile, ul-

tra-pure 0.1M hydrochloric acid, in order to obtain sterile, endotoxin-free solution of Ga-68 chloride. For labelling a vial containing 20ug sterile and endotoxin-free lyophilisate of PSMA-11 (GMP) (ABX, Radeberg, Germany) and a vial containing 60 mg of sodium acetate was used. To the above set 2ml of Ga-68 chloride was added and mixed for 10-20s. to complete dissolution. Subsequently, the mixture was incubated for 10 min. at 95°C. The labelled tracer was purified on a column of Sep-Pak Light C18 (Waters) and filtered on a 0.22 μm pore size filter (MILLEX-GV, Merck). Radiochemical purity (≥95%) was confirmed by thin-layer chromatography, checked on iTLC-SG bands in ammonium acetate-methanol (1:1) solution.

To reduce patients discomfort during the long PET/MR examination time, the patient's arms were placed alongside the body. PET and MR imaging were performed simultaneously. MR sequences included: axial T2-wighted TSE fat-saturated 5mm-slice, 400mm field-of-view (FOV) images, respiratory gated in the region of the chest and abdomen, axial T1-weighted Vibe Dixon 3mm-slice, 430mm FOV images, breath-holded in the region of the chest and abdomen. Attenuation correction was calculated according to the manufacturer's protocol basing on a fast 3D FLASH based MR VIBE (volume interpolated breath-hold examination) sequence.

PET imaging was performed with an acquisition time of 5 min per bed position in caudocranial direction starting from the pelvis. Acquired PET sinograms were reconstructed with the HD-PET algorithm (point-spread function) using 3 iterations, 21 subsets, a Gaussian filter: the Full Width at Half Maximum (FWHM) 4.0 mm, an image matrix of 172. Performed separately, pelvis and lower limbs PET/MR imaging were not analyzed in the current study.

Image analysis

Retrospective analysis of ^{68}Ga-PSMA-11 PET/MR scans, fused and not-fused, included the estimation of the radiotracer uptake (SUV_{max} normalized by body weight) and morphologic features (the size, shape and position) of CTG complex, as well as the symmetry of their location and symmetry of visual uptake intensity. Analysis and quantification was performed on a Syngo.via Viewer workstation (Siemens, Germany).

We used the name "cervico-thoracic ganglia complex" (CTG-C) for the complex of ganglia located in the typical area (described in the discussion), because it is not possible to ascertain reliably on a whole-body MR part of a PET/MR scan if the detected ganglia structures are fused or not, as it is not possible to follow the whole sympathetic chain. The observed complex of ganglia connected by visible strands, possibly included sometimes a T2 sympathetic ganglion or a vertebral ganglion.

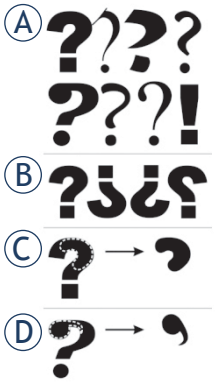

FIGURE 2. Schematic presentation of the discovered in current study "typical" cervico-thoracic ganglia complexes shapes resembling different forms of a question-mark or close to an exclamation-mark **(A)**, which may be configured in various orientations, for example normal, mirror, upside-down and reversed mirror **(B)** or represent a part of a question-mark similar to kidney **(C)** or comma **(D)**.

Asymmetry of PSMA-ligand uptake in CTG-C (in intensity, in the level of maximal intensity, or both), as well as increased uptake in visual assessment and independently, when SUV_{max} amounted at least 2, were regarded as risk factors of mistaking CTG-C for metastases or other malignant lesions. The background ^{68}Ga-PSMA-11 activity was measured in gluteal muscles (GM).

The analysis of the CTG-C shape consisted of two steps. First, the form of all CTG-C was characterized descriptively. Subsequently, the described configurations were reevaluated and categorized. When reviewing CTG complexes we noticed repeating configurations, not previously identified, resembling the shape of a question-mark (thinner or thicker, normal, reversed, mirror or upside-down, more or less straight including bludgeon-like shape), or a part of a question-mark similar to a kidney or comma, as well as exclamation-mark forms (Figure 2). These shapes were categorized as "typical".

The tumor-like shapes: oval, binodular or longitudinal, were regarded as "mistakable", potentially suspicious of malignancy, including lymph node metastasis.

The non-specific shapes (wavy with small nodules, bent or unreliable to be assessed), were named "other", and were also treated as not suspicious of malignancy.

TABLE 1. Dimensions of the right and left cervico-thoracic ganglia complex (CTG-C)

	thickness (mm)			width (mm)			length (mm)		
	Mean ± SD*	minimal	maximal	Mean ± SD	minimal	maximal	Mean ± SD	minimal	maximal
right CTG-C (n = 103)	4.31 ± 1.17	1.5	8	12.50 ± 5.30	4	28	12.7 ± 3.88	5	25
left CTG-C(n = 106)	4.35 ± 1.24	2	8	14.90±4.79	5	29	13.50 ± 3.53	7	25

* SD standard deviation

TABLE 2. ^{68}Ga-PSMA-11 uptake in the right and left cervico-thoracic ganglia complex (CTG-C)

	^{68}Ga-PSMA-11 uptake (SUV_{max})				
	mean	median	SD*	minimal	maximal
right CTG-C	2.54	2.45	0.82	1.06	6.23
left CTG-C	2.75	2.74	0.78	1.35	5.73

* SD standard deviation

Statistical analysis

Statistical calculations were performed using IBM SPSS Statistics for Windows, Version 23.0. Armonk, NY: IBM Corporation (Released 2015). Basic descriptive statistics was calculated and subsequently the Kolmogorov-Smirnov tests, the Pearson's r correlation and $\chi 2$ tests were performed. The significance level of $\alpha = 0.05$ ($p < 0.05$) was selected. The assessed variables included the patients' age (years), height (cm), weight (kg), radiotracer dose (MBq), uptake time (min), background in the GM (SUV_{max}), PSMA-ligand uptake in the right (R) CTG-C and the left (L) CTG-C (SUV_{max}), dimensions (thickness, width, length) of the R-CTG-C and L-CTG-C (mm) for basic descriptive statistics. Normality assumption was verified for variables intended for further correlations (*i.e.* the thickness and SUV_{max} values of CTG-C). Distributions of the thickness of the CTG-C, as well as SUV_{max} values of the right CTG-C and both CTG-C were not normal (differed from the Gaussian distribution). Therefore, verification of the level of skewness of these distributions was advised. The value of skewnees in all variables ranged from -2 to +2, meaning that the distributions were not highly asymmetrical. Therefore, if other assumptions were met, parametric analyses were performed. The correlation between thickness of CTG-C and SUV_{max} was investigated by means of a series of Pearson's r correlation analyses.

In order to check how recognizing the shape of CTG-C as not-suspicious, *i.e.* "typical" or "other", basing on MR, enhanced the accuracy of CTG-C proper identification in comparison with assessment based solely on PET, a series of $\chi 2$ analyses were performed. There were also additional calculations for "typical" shape carried out separately.

Results

On whole-body MR scans the CTG-C was identifiable in 100% on the left (L) side and in 97% (103/106) on the right (R) side, and were located symmetrically or partially symmetrically in 90% (95/106) of patients.

The mean thickness of the CTG-C, *i.e.* minimal transverse diameter, was 4.31 ± 1.20 mm (range, 1.5–8 mm), mean width, *i.e.* maximal diameter on a transverse MR plane, was 13.7 ± 5.18 mm (range, 4–29 mm) and mean length (in cranio-caudal orientation) was 13.1 ± 3.72 mm (range, 5–25 mm). Diameters with respect to the right and left side are presented in Table 1.

All identified CTG-C showed ^{68}Ga-PSMA-11 uptake, with mean SUV_{max} 2.65 ± 0.8 (range 1.06–6.23). Uptake values with respect to the right and left side are presented in Table 2.

With regard to the left CTG-C, there was a positive correlation of a medium size ($r = .318$; $p = .001$) between its thickness and SUV_{max}. Analysis regarding CTG-C of both sides taken together revealed a positive, statistically significant and small-size correlation with SUV_{max} ($r = .179$; $p = .01$). As for the right CTG-C, no correlation nor tendency was found between the thickness and SUV_{max} ($r = .028$; $p = .782$).

Noticeably increased, possible to be taken for malignant, ^{68}Ga-PSMA-11 uptake, $SUV_{max} \geq 2$, was detected in 87.7% (93/106) of the L-CTG-C and 74.5% (79/106) of the R-CTG-C (with respect to both sides see Figure 3); whereas the background in gluteal muscles presented mean SUV_{max} of 1.04 ± 0.32 (range, 0.46–1.81). In visual assessment, as routinely performed in clinical practice, suspicious of malignancy appearance of CTG-C was observed in

70.8% of the L-CTG-C (75/106) and 60.4% (64/106) of the R-CTG-C (with respect to both sides see Figure 3). The main criteria of possible malignancy on PET were the PSMA-ligand avidity and asymmetry of uptake (in the intensity, in the level of maximum intensity or both) in CTG-C (Figure 1B-D; Figure 3A,B; Figure 4A-D).

On MR part of the whole-body PET/MR, in the majority of patients (66.0% L-CTG-C, 70/106; 53.8% R-CTG-C, 57/106), the CTG complex presented the following shapes, reflecting their anatomic structure and connections: a question-mark (L-CTG-C: 23.6%, 25/106; R-CTG-C: 22.6%, 24/106), an exclamation-mark (L-CTG-C: 3.8%, 4/106; R-CTG-C: 2.8%, 3/106), or a part of a question-mark resembling kidney (L-CTG-C: 27.4%, 29/106; R-CTG-C: 12.3%, 13/106) or comma (L-CTG-C: 11.3%, 12/106; R-CTG-C: 16.0%, 17/106) (Figure 3E, F; Figure 5).

The tumor-like CTG-C shape, possible to be mistaken for malignancy, was detected in 28.3% (30/106) on the left side and in 40.6% (43/106) on the right side, probably due to MR artifacts obscuring finer linear elements of the CTG-C and not allowing for the tracing of the entire CTG-C tract (Figure 3C, D). The rest (L-CTG-C: 5.7%, 6/106; R-CTG-C: 5.7%, 6/106) of CTG-C presented non-specific shape.

In cases, where visual molecular assessment of PET revealed suspicious, potentially mistakable with malignancy, increased PSMA-ligand uptake in CTG-C, the recognition of a "typical" or an "other" shape of underlying CTG-C on MR part of the examination generated a rise in the accuracy of their proper identification. For the right CTG-C from 39.6% to 76.4%, $\chi2(1) = 29.46$; $p < .001$, for the left CTG-C from 29.2% to 77.4%, $\chi2(1) = 49.29$; $p < .001$, for both from 34.4% to 76.8%, $\chi2(1) = 77.41$; $p < .001$. The effect size was moderately large, with V = .37, V = .48 and V = .43 for the right, left and both CTG-C, respectively. Recognizing the shape of the CTG-C as a "typical" or an "other" in MR allowed us to classify as "not-suspicious" 60.9% of the right CTG-C, 68% of the left CTG-C and 64.7% of all CTG-C which were treated as "suspicious" after sole PET assessment.

In the separated evaluation of the "typical" MR CTG-C shape the rise in accuracy was from 39.6% to 76.4%, $\chi2(1) = 29.46$; $p < .001$ for the right CTG-C, from 29.2% to 73.6%, $\chi2(1) = 41.71$; $p < .001$ for the left CTG-C, from 34.4% to 75%, $\chi2(1) = 70.4$; $p < .001$ for both. The effect size was moderately large, with V = .37, V = .44 and V = .41 for the right, left and both CTG-C, respectively. Recognizing the shape of the CTG-C as "typical" in MR allowed us to classify as "not-suspicious" 60.9% of the right CTG-C, 62.67% of the left CTG-C and 61.9% of all CTG-C which were treated as "suspicious" after sole PET assessment.

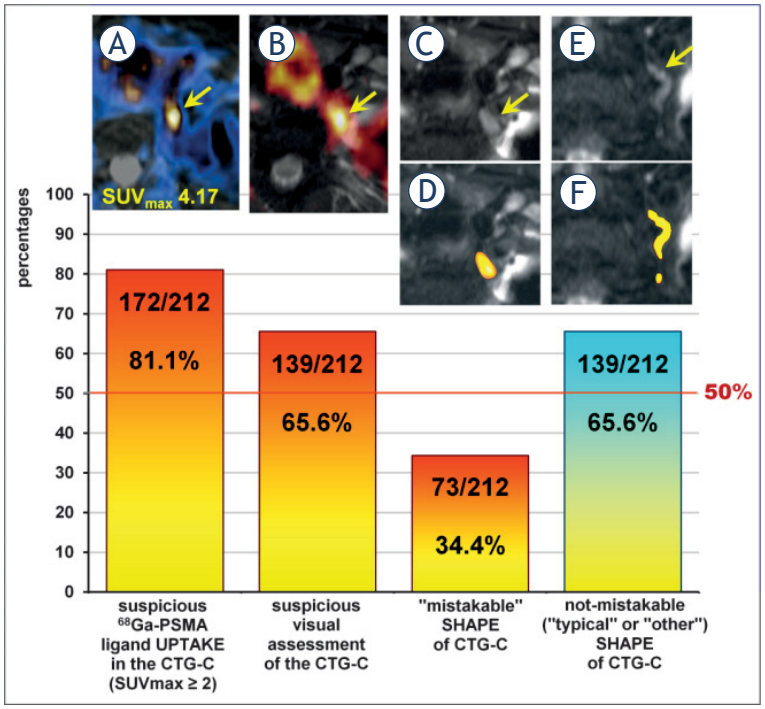

FIGURE 3. The chart comparing proportions of suspicious of malignancy PET presentation of cervico-thoracic ganglia complex (CTG-C) (arrow) in quantitative (SUV_{max} at least 2) and qualitative (visual) assessment with potentially "mistakable" and not-mistakable with malignancy underlying shape of CTG-C on MR part of the multimodal PET/MR. **(A, B)** Fused PET/MR scans of the left CTG-C potentially suspicious of malignancy in different patients. MR T2-weighted scans showing the mistakable (oval) shape **(C)** and not-mistakable (question-mark) shape **(E)** of the left CTG-C (arrow) with respective schemes **(D, F)**.

Discussion

The CTG/SG can be identified along the sympathetic chain on the border between the neck and thorax, anteriorly and slightly caudad to the head of the first rib[11,12], inferior and anterior to the transverse process of C7[12,19], lateral and posterior to the lateral edge of the longus colli muscle (at the level of T1)[11], inferior to the subclavian artery[12], medial, posterior, medial and anterior or medial and posterior to the vertebral artery[3,11]. Which was confirmed also in the current study.

In our study we have tracked down a configuration of the cervico-thoracic ganglia complex not categorized in previous MR study exploring CTG/SG.[11,19] The majority of CG-C in our work resem-

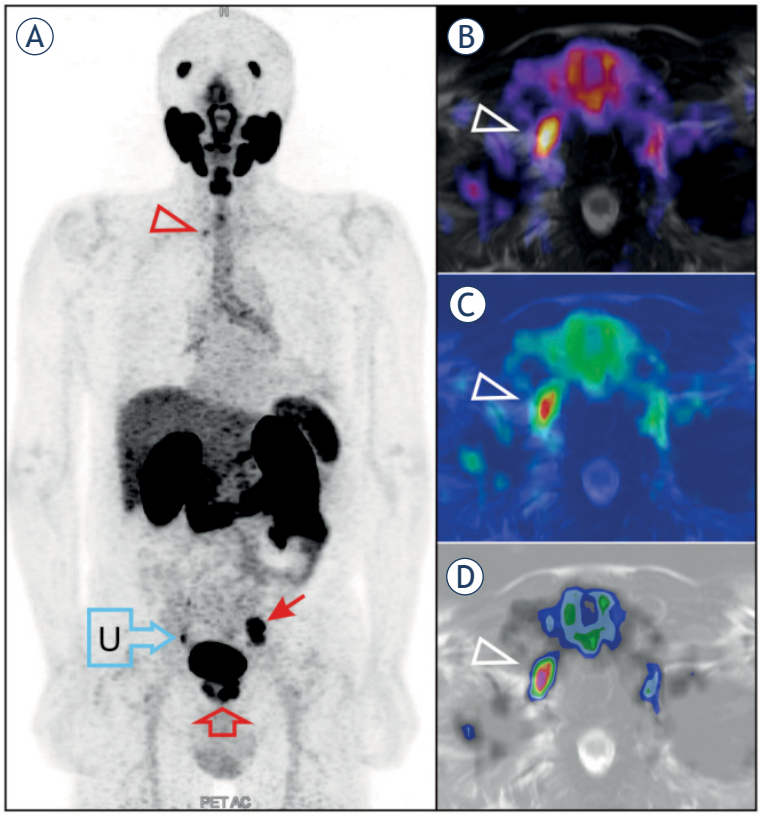

FIGURE 4. (A) Prostate cancer (empty block arrow) with lymph node metastases (arrow) on the maximum intensity projection (MIP) attenuation corrected (AC) PET image. Possibly suspected of metastasis asymmetric increased uptake in the right cervico-thoracic sympathetic ganglion (arrowhaed) is noticeable already on the MIP image **(A)** and more conspicuously on fused PET/MR T2-weighted images presented with application of different color maps **(B-D).**

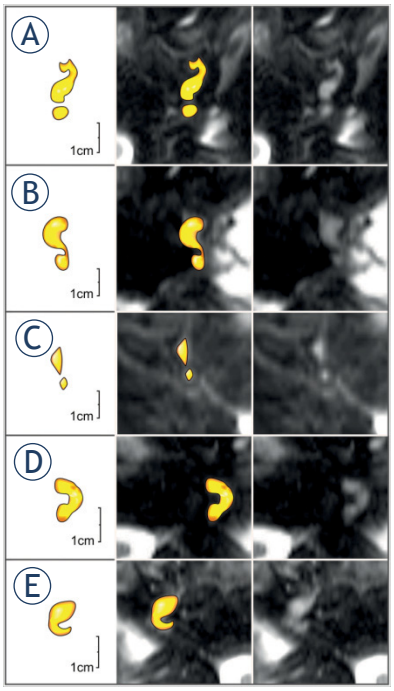

FIGURE 5. Schemes (two first columns) and original MR T2-weighted fat-saturated images (two last columns) depicting exemplary "typical" shapes of the cervico-thoracic ganglia complex (CTG-C): a question-mark shape **(A)**, a mirror question-mark shape **(B)**, an exclamation-mark shape **(C)**, a part of a question-mark resembling kidney **(D)**, a part of a question-mark resembling comma **(E)**.

bled a question-mark in various configurations: thinner or thicker, mirror, reversed or mirror and upside-down, more or less straight including bludgeon-like shape and an exclamation-mark, or a part of a question-mark: without a dot, resembling kidney or comma. Our "dot" in the question-mark or exclamation-mark sign might be T1 sympathetic ganglion (when CTG is not fused) or T2 ganglion (when CTG is fused) in case of a normal or a mirror shape, or a vertebral ganglion – in case of an upside-down appearance.

Even the oval, binodular or longitudinal shapes, classified as tumor-like, were usually partially surrounded by unsuccessful fat saturation artifacts, which probably obscured the finer sympathetic branches or chain and in more favorable conditions might let the recognition of a "typical" shape.

Many of presented in our work shapes or their parts correspond to the shapes described previously on CT or anatomical studies.[15]

On CT it is not possible to trace fine structures as nerves and their connections, therefore only thicker oval or longitudinal parts of a neuronal network are identifiable. That is the reason why MR-based multimodal PET/MR, which can depict strand of the sympathetic chain, may be more specific in identifying sympathetic ganglia. Nevertheless, the data available with PET/CT have been already proved to be entirely sufficient for correct interpretation of findings.[15]

The analysis of the CTG-C shape appears important in the context of potentially suggesting metastasis or other malignancy PSMA-ligand uptake on multimodal PET/MR, which was present in our study in 65.6% in visual assessment and in 81.1% when regarding abnormal SUV_{max} of at least 2. We have chosen the SUV_{max} 2, because it was used also in some previous papers as a cut-off value for prostate cancer metastases[16,20,21] and because it constitutes the reported lower range in lymph nodes metastases in prostate cancer[14,22], as well as it exceeded the upper range of the background SUV_{max} (1.81) in our study.

Elevated PSMA-ligand uptake in CTG/SG may be properly recognized as not alarming under a few conditions. The most important of them is awareness of the diagnostic reader that such a possibility exists, second is the typical location, subsequently – symmetry. The listed aspects were already underlined by authors of PET/CT studies.[13,15] Further aspects, including the likelihood on prostate cancer metastases on the level of the cervico-thoracic junction and the intensity of prostate cancer metastases[15] are discussed below.

We have observed, that morphological symmetry of CTG-C location (beginning and ending on the same or very similar level) did not necessarily overlap with the point of maximal PSMA-ligand uptake, therefore morphologically symmetric CTG-C seemed often to have asymmetric foci of maximal uptake when viewed on fused PET/MR images, facilitating a diagnostic mistake. Therefore, the additional observation of a specific underlying MR shape below the suspicious uptake on PET constitutes the additional useful tip aiding proper diagnosis. Reasons for asymmetry of CTG-C location on MR might include also, apart from true anatomic asymmetry, the asymmetric patient position resulting in the transverse MR plane not exactly perpendicular do the true long axis of the body.

Rischpler *et al.*[15] in the ample PET/CT study reported cervical sympathetic ganglia as having often a characteristic band-shaped (57.5%) and tear-drop (38.5%) configuration. The band-shape may reflect described in our current study elements of a question mark and a tear-drop may be close to our comma shape.

Shapes of SG described in MR-based study encompassed: fusiform, triangular, or globular but concerned only 9 volunteers.[11]

Shapes of SG described in anatomical cadaver studies included: spindle, dumbbell, and an inverted "L" shape (with the two latest demonstrating a definite "waist")[7], to which Marcer *et al.*[6] had added a perforated (by the vertebral artery usually at the superior portion) and a truncated form (where the vertebral artery created a shortened and flattened form of the ganglion). Kwon *et al.*[5] categorized SG shapes as fusiform-rounded, fusiform-elongated, and bilobed.

However, the shapes assessed basing on dissection studies may be deprived of their fine spacial arrangement visible on MR, but lost during preparation. The choice of the classification is subjective and may be free and depends on the imagination of the author. Comparing between pathology and imaging bears the burden of different condition of the organism at the time of examination, and therefore the results may be difficult to equate. The overall better tissue delineation on MR does not take the general diagnostic sufficiency away from CT.

The binodular shape in our study may reflect anatomically described dumbbell or bilobed form. The fusiform shape after dissection may lose its bent projection depicted on MR in the form of a question-mark. The truncated or "L" shape form probably might partially correspond to the kidney shape on MR. The association of CTG-C shape with the "question-mark" does not claim to be a novel discovery of that shape itself, but may better help an unexperienced reader to remember the problem.

Nevertheless, the results of previous papers prove, that data available with application of PET/CT are sufficient to correctly classify sympathetic ganglia on multimodal imaging with PSMA-ligands.[15] Especially that in case of prostate cancer, metastases as high as at the level of CTG-C are not so often and that prostate cancer metastases adjacent to ganglia show significantly more intense PSMA-ligand uptake[15], and we would like to stress the above conclusion.

The thickness range of CTG-C was in our study 1.5–8 mm, whereas Perlov and Vehe (1935) reported 3–10 mm for satellite ganglia. The mean thickness of CTG-C in our study (4.31 mm) was in close concordance with anatomical cadaver studies (4.5 mm by Marcer *et al.*[6]), but smaller than 8 mm reported by Jamieson *et al.*[2] The other diameters also differed in comparison with cadaver studies, the length was shorter, which was most probably caused by the different character of the study method: section – and imaging, and possibly because of different measurement policies and the measurement plane. Similarly, Hogan and Erickson[11] in MR study reported obtaining smaller cephalocaudal SG dimension than in previous dissection studies, of just over 1cm, which corresponded to our results of about 13 mm.

In our MR-based study mean SUV_{max} was similar, and only slightly higher (2.75 in the L-CTG-C and 2.54 in the R-CTG-C) than reported in CT-based multimodal PET studies: by Kanthan *et al.*[13]: 2.4 in the L-CTG-C and 2.2 in the R-CTG-C, and by Rischpler *et al.*[15]: 2.4.

The indisputable and undeniable, however unavoidable shortcoming of current study, identically to previous studies, is the impossibility of reliable confirmation of the true nature of studied ganglia, for obvious reasons of unattainable histopathological result. A few researches in previous works concerning celiac sympathetic ganglia tried to make a restitution for that by examining cadavers with CT or MRI and later performing the HP analysis.[14,23] Their conclusions confirmed the sufficiency of using anatomical landmarks for locating the ganglia.

To sum up, special properties of a novel PET PSMA-based radiotracer, physiologically accumulating also in anatomically normal sympathetic ganglia, including cervico-thoracic ones, impelled researchers to study meticulously all possible prop-

erties of these ganglia to avoid mistaking them for malignancy. In our study we associated discovered detailed anatomical CTG-C shapes with a form of a question-mark, exclamation-mark or a part of a question-mark to facilitate an unexperienced reader proper interpretation of the PSMA-ligand PET/MR examination.

Conclusions

The characteristic shape of the cervico-thoracic ganglia complex (resembling a question-mark or its part), reflecting CTG complex anatomy, helps in proper recognition of CTG-C on multimodal whole-body ^{68}Ga-PSMA-ligand PET/MR imaging, when detectable uptake might lead to considering pathology.

References

1. Raveendran VL, Kamalamma GK. Inferior cervical ganglion and stellate ganglion- concepts revisited. *J Evolution Med Dent Sci* 2018; **7:** 1653-8. doi: 10.14260/jemds/2018/373
2. Jamieson DW, Smith DB, Anson JB. The cervical sympathetic ganglia: an anatomical study of 100 cervicothoracic dissections. *Q Bull Northwest Univ Med Sch* 1952; **26:** 219-27. PMID: 14957979
3. Perlow S, Vehe KL. Variations in the gross anatomy of the stellate and lumbar sympathetic ganglia. *Am J Surg* 1935; **30:** 454-8
4. Hoffman HH. An analysis of the sympathetic trunk and rami in the cervical and upper thoracic regions in man. *Ann Surg* 1957; **145:** 94-103. doi: 10.1097/00000658-195701000-00010
5. Kwon OJ, Pendekanti S, Fox JN, Yanagawa J, Fishbein MC, Shivkumar K, et al. Morphological spectra of adult human stellate ganglia: Implications for thoracic sympathetic denervation. *Anat Rec (Hoboken)* 2018; **301:** 1244-50. doi: 10.1002/ar.23797
6. Marcer N, Bergmann M, Klie A, Moor B, Djonov V. An anatomical investigation of the cervicothoracic ganglion. *Clin Anat* 2012; **25:** 444-51. doi: 10.1002/ca.21266
7. Pather N, Partab P, Singh B, Satyapal KS. Cervico-thoracic ganglion: its clinical implications. *Clin Anat* 2006; **19:** 323-6. doi: 10.1002/ca.20214
8. Duong S, Bravo D, Todd KJ, Finlayson RJ, Tran DQ. Treatment of complex regional pain syndrome: an updated systematic review and narrative synthesis. *Can J Anaesth* 2018; **65:** 658-84. doi: 10.1007/s12630-018-1091-5
9. Przybylski A, Romanek J, Chlebuś M, Deręgowska B, Kuźniar J. Percutaneous stellate ganglion block as an adjunctive therapy in the treatment of incessant ventricular tachycardia. *Kardiol Pol* 2018; **76:** 1018-20. doi: 10.5603/KP.2018.0120
10. Summers MR, Nevin RL. Stellate ganglion block in the treatment of posttraumatic stress disorder: a review of historical and recent literature. *Pain Pract* 2017; **17:** 546-53. doi: 10.1111/papr.12503
11. Hogan QH, Erickson SJ. MR imaging of the stellate ganglion: normal appearance. *AJR Am J Roentgenol* 1992; **158:** 655-9. Erratum in: *AJR Am J Roentgenol* 1992; **158:** 1320. doi: 10.2214/ajr.158.3.1739014
12. Beheshti M, Rezaee A, Langsteger W. 68Ga-PSMA-HBED uptake on cervicothoracic (Stellate) ganglia, a common pitfall on PET/CT. *Clin Nucl Med* 2017; **42:** 195-6. doi: 10.1097/RLU.0000000000001518
13. Kanthan GL, Hsiao E, Vu D, Schembri GP. Uptake in sympathetic ganglia on 68Ga-PSMA-HBED PET/CT: a potential pitfall in scan interpretation. *J Med Imaging Radiat Oncol* 2017; **61:** 732-8. doi: 10.1111/1754-9485.12622
14. Krohn T, Verburg FA, Pufe T, Neuhuber W, Vogg A, Heinzel A, et al. [(68)Ga]PSMA-HBED uptake mimicking lymph node metastasis in coeliac ganglia: an important pitfall in clinical practice. *Eur J Nucl Med Mol Imaging* 2015; **42:** 210-4. doi: 10.1007/s00259-014-2915-3
15. Rischpler C, Beck TI, Okamoto S, Schlitter AM, Knorr K, Schwaiger M, et al. 68Ga-PSMA-HBED-CC uptake in cervical, coeliac and sacral ganglia as an important pitfall in prostate cancer PET imaging. *J Nucl Med* 2018; **59:** 1406-11. doi: 10.2967/jnumed.117.204677
16. Giesel FL, Fiedler H, Stefanova M, Sterzing F, Rius M, Kopka K, et al. PSMA PET/CT with Glu-urea-Lys-(Ahx)-[^{68}Ga(HBED-CC)] versus 3D CT volumetric lymph node assessment in recurrent prostate cancer. *Eur J Nucl Med Mol Imaging* 2015; **42:** 1794-800. doi: 10.1007/s00259-015-3106-6
17. Giesel FL, Kesch C, Yun M, Cardinale J, Haberkorn U, Kopka K, et al. 18F-PSMA-1007 PET/CT detects micrometastases in a patient with biochemically recurrent prostate cancer. *Clin Genitourin Cancer* 2017; **15:** e497-e9. doi: 10.1016/j.clgc.2016.12.029
18. Bialek EJ, Malkowski B. Celiac ganglia: can they be misinterpreted on multimodal 68Ga-PSMA-11 PET/MR? *Nucl Med Commun* 2019; **40:** 175-84. doi: 10.1097/MNM.0000000000000944
19. Chaudhry A, Kamali A, Herzka DA, Wang KC, Carrino JA, Blitz AM. Detection of the stellate and thoracic sympathetic chain ganglia with high-resolution 3D-CISS MR imaging. *AJNR Am J Neuroradiol* 2018; **39:** 1550-4. doi: 10.3174/ajnr.A5698
20. van Leeuwen PJ, Stricker P, Hruby G, Kneebone A, Ting F, Thompson B, et al. (68) Ga-PSMA has a high detection rate of prostate cancer recurrence outside the prostatic fossa in patients being considered for salvage radiation treatment. *BJU Int* 2016; **117:** 732-9. doi: 10.1111/bju.13397
21. Vinsensia M, Chyoke PL, Hadaschik B, Holland-Letz T, Moltz J, Kopka K, et al. 68Ga-PSMA PET/CT and volumetric morphology of PET-positive lymph nodes stratified by tumor differentiation of prostate cancer. *J Nucl Med* 2017; **58:** 1949-55. doi: 10.2967/jnumed.116.185033
22. Sahlmann CO, Meller B, Bouter C, Ritter CO, Ströbel P, Lotz J, et al. Biphasic ^{68}Ga-PSMA-HBED-CC-PET/CT in patients with recurrent and high-risk prostate carcinoma. *Eur J Nucl Med Mol Imaging* 2016; **43:** 898-905. doi: 10.1007/s00259-015-3251-y
23. Abtahi SM, Elmi A, Hedgire SS, Ho YC, Pourjabbar S, Singh S, et al. Depiction of celiac ganglia on positron emission tomography and computed tomography in patients with lung cancer. *Clin Imaging* 2014; **38:** 292-5. doi: 10.1016/j.clinimag.2013.12.017